Time-Resolved Absorption Studies of Native Etiolated Oat Phytochrome

Chian-Fan Zhang,[†] David L. Farrens,[‡] Sofie C. Björling,[†] Pill-Soon Song,[‡] and David S. Kliger*,[†]

Contribution from the Department of Chemistry and Biochemistry, University of California, Santa Cruz, California 95064, and Department of Chemistry, University of Nebraska, Lincoln, Nebraska 68588. *Received October 7, 1991*

Abstract: The phototransformation kinetics of native oat phytochrome from etiolated seedling shoots of *Avena sativa* was investigated by laser photolysis experiments at 10 °C. The phototransformation from the red-absorbing form (Pr) to the far-red-absorbing form (Pfr) was initiated by 7-ns (fwhm) laser pulses at 638 nm. The transient absorption difference spectra in the UV and visible regions were recorded from 100 ns to 800 ms after photolysis by a gated optical multichannel analyzer system. A global fitting procedure employing a singular value decomposition method was used to simultaneously analyze the difference spectra at various times after photolysis. The global analysis of the laser photolysis data shows that the phototransformation from Pr to Pfr involves five kinetic intermediates. At 10 °C the apparent lifetimes associated with these intermediates are 7.4 μs, 89.5 μs, 7.6 ms, 42.4 ms, and at least 266 ms. It is possible to fit the transient absorption data with kinetic models involving two parallel pathways or sequential pathways with equilibria at certain stages of the phototransformation. The formation of Pfr involves an unbranched reaction. Discussions of the possible kinetic mechanisms of the phototransformation and the absorption spectra of the intermediates derived from these models are presented.

Introduction

Phytochrome is the primary sensory pigment in green plants which controls a wide variety of developmental and morphogenic processes, including seed germination, biosynthesis of chlorophylls, and flowering.[1-6] At physiological temperatures, the pigment can exist in two stable and photoreversible forms: the inactive, red-absorbing Pr form and the active, far-red-absorbing Pfr form. The formation of Pfr from Pr following absorption of red light triggers many morphogenic responses as well as light-responsive gene expression. Although the mechanism of regulation is unknown at present, some photomorphogenic processes are believed to be regulated by phytochrome actions on gene expression in plants. Native phytochrome in etiolated oat seedling shoots is a 124 kDa soluble protein which forms a dimer in solution near neutral pH. The pigment contains an open tetrapyrrole chromophore which is covalently attached to the Cys-321 residue of the apoprotein through a thioether bond.[7-9] The conformations and configurations of the chromophore in Pr and in Pfr are believed to differ. It is proposed that the open tetrapyrrole in the red-absorbing form of oat phytochrome has a *Z,Z,Z* structure while that in the far-red-absorbing form has a *Z,Z,E* structure.[9-14] Furthermore, it is suggested by the resonance Raman studies that the chromophore in Pr is protonated,[15] while that in Pfr is unprotonated,[16] at the nitrogen of pyrrole ring C. The absorption of red light by the chromophore initiates a photoreaction followed by a series of dark reactions which lead to the active form of the pigment at physiological temperatures. The dark reactions of phytochrome involve a number of metastable intermediates characterized by distinct absorption spectra.[17,18] These intermediates exhibit decay rate constants from microseconds to hundreds of milliseconds.[19] A simplified scheme of the phototransformation of native oat phytochrome, suggested by low-temperature steady-state studies,[18] is shown in Figure 1.

It was observed in picosecond absorption studies that at room temperature the excited state of photolyzed Pr decayed with a lifetime of 40 ps to form an initial intermediate called prelumi-R.[20,21] The first intermediate which can be stabilized at low temperatures,[18] lumi-R, is formed from the initial intermediate within 100 ps at room temperature. These observations are consistent with the excited-state lifetimes of the pigment measured by picosecond fluorescence studies.[22,23] The fact that the fast fluorescence component exhibited a negligible deuterium isotope effect made it unlikely that protein transfer took place in the initial reaction. The tetrapyrrole chromophore is believed to undergo *Z-E* isomerization at the C_{15}-C_{16} double bond in the initial photoprocess.[24,25] However, despite intensive studies on the phototransformation in recent years, the kinetic mechanism of the subsequent dark reactions is still a subject of controversy. The discrepancies in the literature involve the number of kinetic intermediates in the phototransformation as well as how these in-

[†] University of California.
[‡] University of Nebraska.

(1) Song, P.-S. In *Advanced Plant Physiology*; Wilkins, M. B., Ed.; Pitman Books: London, 1984; pp 354-379.
(2) Song, P.-S. *J. Photochem. Photobiol., B* **1988**, *2* (1), 43-57.
(3) Lagarias, J. C. *Photochem. Photobiol.* **1985**, *42*, 811-820.
(4) Furuya, M., Ed. *Phytochrome and Photoregulation in Plants*; Academic Press: Orlando, FL, 1987.
(5) Furuya, M. *Adv. Biophys.* **1989**, *25*, 133-167.
(6) Whitelam, G.; Smith, H. In *Plant Pigments*, Goodwin, T. W., Ed.; Academic Press: London, 1988; pp 257-298.
(7) Lagarias, J. C.; Rapoport, H. *J. Am. Chem. Soc.* **1980**, *102*, 4821-4828.
(8) Hershey, H. P.; Barker, R. F.; Idler, K. B.; Lissemore, J. L.; Quail, P. H. *Nucleic Acids Res.* **1985**, *13*, 8543-8559.
(9) Rüdiger, W. *Photobiochem. Photobiophys.* **1987** (*Suppl. 1987*), 217-227.
(10) Thümmler, F.; Rüdiger, W.; Cmiel, E.; Schneider, S. *Z. Naturforsch.* **1983**, *38c*, 359-368.
(11) Rüdiger, W.; Thümmler, F.; Cmiel, E.; Schneider, S. *Proc. Natl. Acad. Sci. U.S.A.* **1983**, *80*, 6244-6248.
(12) Farrens, D. L.; Holt, R. E.; Rospendowski, B. N.; Song, P.-S.; Cotton, T. M. *J. Am. Chem. Soc.* **1989**, *111*, 9162-9169.
(13) Rospendowski, B. N.; Farrens, D. L.; Cotton, T. M.; Song, P.-S. *FEBS Lett.* **1989**, *258*, 1-4.
(14) Fodor, S. P. A.; Lagarias, J. C.; Mathies, R. A. *Biochemistry* **1990**, *29*, 11141-11146.
(15) Fodor, S. P. A.; Lagarias, J. C.; Mathies, R. A. *Photochem. Photobiol.* **1988**, *48*, 129-136.
(16) Tokutomi, S.; Mizutani, Y.; Anni, H.; Kitagawa, T. *FEBS Lett.* **1990**, *269*, 341-344.
(17) Kendrick, R. E.; Spruit, C. J. P. *Photochem. Photobiol.* **1977**, *26*, 201-214.
(18) Eilfeld, P.; Rüdiger, W. *Z. Naturforsch.* **1985**, *40c*, 109-114.
(19) Inoue, Y.; Rüdiger, W.; Grimm, R.; Furuya, M. *Photochem. Photobiol.* **1990**, *52*, 1077-1083.
(20) Lippitsch, M. E.; Riegler, H.; Aussenegg, F. R.; Hermann, G.; Muller, E. *Biochem. Physiol. Pflanzen.* **1988**, *183*, 1-6.
(21) Song, P.-S.; Sarkar, H. K.; Kim, I.-S.; Poff, K. L. *Biochmim. Biophys. Acta* **1981**, *635*, 369-382.
(22) Brock, H.; Ruzsicska, B. P.; Holzwarth, A. R.; Braslavsky, S. E.; Arai, T.; Schlamann, W.; Schaffner, K. *Biochemistry* **1987**, *26*, 1412-1417.
(23) Song, P.-S.; Singh, B. R.; Tamai, N.; Yamazaki, T.; Yamazaki, I.; Tokutomi, S.; Furuya, M. *Biochemistry* **1989**, *28*, 3265-3271.
(24) Eilfeld, P.; Eilfeld, P.; Rüdiger, W. *Photochem. Photobiol.* **1986**, *44*, 761-769.
(25) Hermann, G.; Lippitsch, M. E.; Brunner, H.; Aussenegg, F. R.; Muller, E. *Photochem. Photobiol.* **1990**, *52*, 13-18.

0002-7863/92/1514-4569$03.00/0

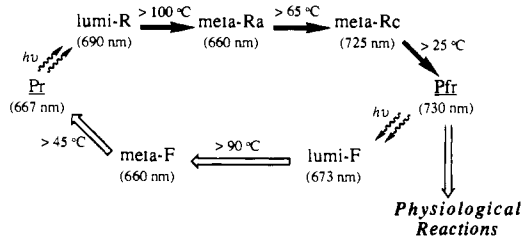

Figure 1. Scheme of phytochrome phototransformation suggested from low-temperature steady-state absorption studies by Eilfeld and Rüdiger.[18] The approximate room-temperature absorption maxima of the species are given in parentheses below each intermediate, and the temperatures below which the indicated transformation is blocked are indicated above the relevant arrows.

termediates are interconnected. From their low-temperature steady-state measurements on native oat phytochrome, Eilfeld and Rüdiger found three intermediates (called lumi-R, meta-Ra, and meta-Rc) in the phototransformation from Pr to Pfr.[18] Their transient absorption studies at room temperature were interpreted to suggest that the photointermediates decay in a simple sequential pathway.[26] However, other kinetic absorption measurements, such as double-flash studies, suggest that the phototransformations of native and large (i.e., 114/118 kDa) phytochromes should be interpreted by more complicated mechanisms involving parallel pathways.[27-33] More recently, Eilfeld and co-workers proposed that the phototransformation of native oat phytochrome involves parallel decay of the early intermediates but sequential decay of the latter intermediates.[34] The most recent work of Inoue et al. establishes that the forward phototransformation of native oat phytochrome involves four kinetic intermediates.[19] However, it is not clear how these intermediates are interrelated.

The discrepancies found in the previous studies on the phytochrome phototransformation could be due to different experimental conditions, such as the temperatures at which the experiments were performed or the sample conditions, as well as due to the differences in the methods of data analysis. In most previous studies (except refs 26 and 34), kinetic measurements were carried out and analyzed separately at different wavelengths. This limitation could conceivably contribute to some inconsistencies in the results obtained at different wavelengths. The comparison of the kinetic results at different wavelengths could be quite perplexing since the absorption change at a particular wavelength could be quite significant at a certain stage of the dark reactions but not at other stages (see ref 35, for example). Furthermore, kinetic absorption measurements at a few wavelengths are usually not sufficient to determine spectra of the intermediates and to resolve the mechanism of the phototransformation. In more recent studies, transient absorption spectra were obtained at a few select delay times to obtain the spectra of the phytochrome intermediates.[19,34,36] Each of the transient spectra probably resulted from the absorption of multiple intermediates rather than a unique intermediate. It should be pointed out that it can be misleading to interpret the mechanism of phototransformation using these convoluted spectra since, as will be shown in the Global Data Analysis and Results sections, it is possible to explain the same transient data by a number of different kinetic models.

In order to overcome the limitations in the previous studies, we adopted a systematic approach for analyzing the transient spectral data which has allowed us to study the different models of the phytochrome phototransformation in greater detail. We performed time-resolved absorption measurements on the forward phototransformation (from Pr to Pfr) of native oat phytochrome at 10 °C and obtained transient difference absorption spectra at delay times from 100 ns to 800 ms following laser photolysis. We then used a global fitting algorithm to simultaneously analyze the difference spectra at various delay times to determine the absorption changes at different wavelengths which obey the same kinetics. The global analysis of our data was carried out with the aid of a singular value decomposition (SVD) method, which significantly simplified the data matrix used for the fitting procedures.[37,38] We also extended the measurements to the transient absorption changes of the pigment in the near-UV and blue spectral regions at a few select delay times after photolysis. We present here the results of these measurements and the global analysis of the time-resolved spectral data in the red spectral region along with a discussion of possible kinetic mechanisms of the phototransformation and the absorption spectra of the intermediates derived from these models.

Experimental Section

Materials and Experimental Methods. Native 124 kDa phytochrome samples used in the present study were isolated and purified from etiolated oat seedling shoots (*Avena sativa* L. cv. Garry oat). The procedures of sample preparation have been described in detail elsewhere.[39] The sample was solubilized in potassium phosphate buffer solution at pH 7.8. To stabilize the sample, 1 μg per milligram of phytochrome leupeptin and about 5% (w/w) glycerol were added. The specific absorbance ratio of the sample ($A(667)/A(280)$ of Pr) used in all the experiments was 0.82. This ratio was reduced to about 0.65 at the end of the experiments due to the increased sample scattering in the UV region (see more details below). The ratio $\Delta A(667)/\Delta A(730)$ was 1.1 in the difference absorption spectrum of Pfr and Pr, indicating that the phytochrome sample used was in the native form. Samples of 1 mg/mL concentration were flowed by a peristaltic pump between a flask reservoir kept in an ice bath and an optical cell of 1-cm pathlength. The optical density of the Pr form in the cell was approximately 0.8 at 667 nm. The cell had four quartz optical windows and was stabilized at 10 °C to keep the sample stable in the native form and to avoid frost on the cell windows throughout the long experimental period.

The sample was photolyzed by 7-ns (fwhm), 3-mJ actinic laser pulses from a Quanta Ray DCR-2 Nd:YAG pumped dye laser (Spectra-Physics, Mountain View, CA). The actinic laser pulse was at 638 nm with a 10-nm bandwidth due to the contribution of asymmetrical spontaneous emission (ASE) from the DCM dye (Exciton, Dayton, OH). The transient spectral change of the sample was monitored by a pulsed xenon flashlamp probe light source and a gated optical multichannel analyzer (OMA).[40] The actinic laser beam entered the sample at 90° from the probe flashlamp beam, and the polarization of the probe beam was set at the magic angle (54.7°) from that of the actinic beam to avoid optical artifacts due to the rotational relaxation of the pigment following polarized light excitation. The flashlamp intensity was low enough that its photochemical effect on the sample was negligible. The broadband spectral output of the probe pulse was dispersed by a Monospec 27 spectrograph (Thermo Jarrell Ash, Franklin, MA) with a 150 grooves/mm grating before entering the OMA detector. The entrance slit width was set to 150 μm, providing a spectral resolution of approximately 3 nm. For measurements in the red spectral region a red-sensitive OMA detector (Model 1420RT, EG&G, PARC, Princeton, NJ) was used with a pulse amplifier (Model 1304, EG&G) which provided sampling pulses of 500-ns gatewidth. The spectral measurements were taken at logarithmic delay times with 10 points in each time decade from 1 μs to 800 ms. The delay times approximately obeyed the relationship of $t_{n+1} = 1.25t_n$. The spectral measurements between 100 ns and 1 μs were taken at five delay times of 100, 160, 250, 400, and 630 ns. Therefore,

(26) Eilfeld, P.; Eilfeld, P.; Vogel, J.; Maurer, R. *Photochem. Photobiol.* **1987**, *45*, 825-830.
(27) Pratt, L. H.; Butler, W. L. *Photochem. Photobiol.* **1970**, *11*, 361-369.
(28) Pratt, L. H.; Inoue, Y.; Furuya, M. *Photochem. Photobiol.* **1984**, *39*, 241-246.
(29) Braslavsky, S. E. *Pure Appl. Chem.* **1984**, *56*, 1153-1165.
(30) Cordonnier, M.-M.; Mathis, P.; Pratt, L. H. *Photochem. Photobiol.* **1981**, *34*, 733-740.
(31) Inoue, Y.; Furuya, M. *Plant Cell Physiol.* **1985**, *26*, 813-819.
(32) Krieg, M.; Aramendia, P. F.; Braslavsky, S. E.; Schaffner, K. *Photochem. Photobiol.* **1988**, *47*, 305-310.
(33) Scheuerlein, R.; Inoue, Y.; Furuya, M. *Photochem. Photobiol.* **1988**, *48*, 519-524.
(34) Eilfeld, P.; Vogel, J.; Maurer, R.; Eilfeld, P. *J. Photochem. Photobiol. B: Biol.* **1989**, *3*, 209-222.
(35) Ruzsicska, B.; Braslavsky, S. E.; Schaffner, K. *Photochem. Photobiol.* **1985**, *41*, 681-688.
(36) Shimazaki, Y.; Inoue, Y.; Yamamoto, K. T.; Furuya, M. *Plant Cell Physiol.* **1980**, *21*, 1619-1625.
(37) Golub, G. H.; Reinsch, C. *Numer. Math.* **1970**, *14*, 403-420.
(38) Golub, G. H.; Pereyra, V. *J. Numer. Anal.* **1973**, *10*, 413-432.
(39) Chai, Y. G.; Singh, B. R.; Song, P.-S.; Lee, J.; Robinson, G. W. *Anal. Biochem.* **1987**, *163*, 322-330.
(40) Lewis, J. W.; Yee, G. G.; Kliger, D. S. *Rev. Sci. Instrum.* **1987**, *58*, 939-944.

spectra at a total of 65 times following photolysis were measured in the red spectral region. The effects of using a 500-ns OMA gate on results from the early time data will be discussed in the Discussion section below. Since both the intensity of the flashlamp and the detector sensitivity of the OMA declined dramatically in the near-infrared region, a number of yellow plastic color filters were used to dramatically reduce the flashlamp light intensity between 500 and 600 nm so that a relatively uniform intensity profile was recorded by the OMA between 550 and 850 nm. This is particularly important in the present study because a reliable baseline correction of the spectra (achieved by setting the difference spectra between 830 and 850 nm to zero) and a relatively uniform signal/noise ratio in the spectral region of interest are critical to the reliability of the global analysis of the data. Since the spectral data at different times were obtained in separate measurements in this work, the baseline drift during the measurements could contribute additional noise to the kinetic data. Therefore, it is important to obtain "clean" baselines between 830 and 850 nm at which the difference absorption signal is zero at any delay times. For the measurements in the UV–blue spectral region, a blue-sensitive OMA detector (Model 1420, EG&G) was used with a pulse generator (Model AVL-2A-PS-W-N, Avtech Electrosystems Ltd., Ogdensburg, NY) which provided 100-ns sampling pulses. The measurements here were taken at only one point per time decade. A few green plastic filters and a solution filter of concentrated rose bengal were used to provide an even probe intensity distribution between 300 and 500 nm.

To perform the photolysis experiments, a single transient difference spectrum of the pigment was recorded at specific delay times after every photolysis event. After each photolysis pulse, the sample was flowed and illuminated by a cw lamp (Model 9741-50, Cole Parmer Instruments, Chicago, IL) entering the cell from the opposite direction of the actinic beam for about 20 s in order to photochemically convert the photolyzed sample back to Pr. A HOYA R-72 filter was placed between the sample and the cw lamp to ensure that the illumination was at wavelengths above 730 nm. In order to ensure that the sample temperature was stabilized at 10 °C, the sample was then left in the cell (without flowing) for approximately another 10 s before the cw lamp was turned off and the next photolysis measurement made. The complete reversion of the photolyzed sample to the Pr form was shown by the fact that the difference spectrum between the unphotolyzed and photolyzed samples after cw illumination was flat between 550 and 850 nm. The transient difference absorption spectra were collected from 100 ns to 800 ms following photolysis of Pr. An entire set of measurements in the red spectral region (16 averages at 65 different delay times) took about 10 h and that in the near-UV region (about 70 averages at 8 different times) about 6 h to collect. The bleaching and the scattering of the sample due to laser photolysis were checked at the end of the experiment and were found to be less than 10% of the absorption band of the fresh pigment. The transient difference absorption spectra at 100 ns and 100 ms after photolysis measured near the end of the experiment were found to be identical, within the noise level, to that measured at the beginning of the experiment. These results indicate that the native phytochrome sample is stable during the entire period of the measurement. However, our measurements at different delay times were still taken in an alternating sequence to avoid systematic errors due to any change of experimental conditions over the prolonged period of the experiment. The absorption spectra in the red spectral region were analyzed by singular value decomposition (SVD) and a global exponential fitting routine which uses a Simplex algorithm. All data analyses were performed on a Sun Workstation (Sun SPARC Server 390, Sun Microsystems, Inc., Mountain View, CA) using Matlab software (Pro-Matlab, The Math Works, Inc., South Natick, MA).

Global Data Analysis. For a unimolecular reaction involving N kinetic intermediates, where each decays to other intermediate(s) or the final product with different rate constant(s), the time evolution of the concentrations of these intermediates can be described by a set of first-order, linear differential equations. The solution of these equations depends not only on the rate constants of the decay processes but also on how the intermediates are interconnected. In general, it contains a linear combination of N exponentials, each representing a decay process characterized by a different apparent rate constant. For a unidirectional unbranched reaction, for example, the time dependence of the concentration of the ith intermediate (C_i) is given by[41]

$$C_i(t) = C_0\left(\prod_{j=1}^{i-1} k_j\right)\sum_{j=1}^{i}\frac{\exp(-k_j t)}{\prod_{h\neq j;\,h=1;i}(k_h - k_j)} \qquad (1 \le i \le N) \tag{1}$$

(41) Nagle, J. F.; Parodi, L. A.; Lozier, R. H. *Biophys. J.* **1982**, *38*, 161–174.

where C_0 is the initial concentration of the photolyzed species at $t = 0$ and k_j and k_h are the apparent rate constants of the jth and hth processes, respectively. Generally, concentrations of the intermediates at any time, t, can be expressed as

$$\mathbf{C} = C_0\mathbf{K}\mathbf{T} \tag{2}$$

where $\mathbf{C} = \{C_1(t), C_2(t), ..., C_N(t), C_{N+1}(t)\}^T$, $\mathbf{T} = \{\exp(-k_1 t), \exp(-k_2 t), ..., \exp(-k_N t), 1\}^T$, and $\mathbf{K}$ is an $(N + 1) \times (N + 1)$ matrix determined by the mechanism of the reaction and the values of the apparent rate constants, $k_1, k_2, ..., k_N$. Here $C_{N+1}(t)$ represents the concentration of the final reaction product, for which the rate constant $k_{N+1} = 0$ and the matrix or vector $\mathbf{X}^T$ represents the transpose of $\mathbf{X}$. It should be pointed out that the values of the apparent rate constants in eq 1 could be different from those of the "intrinsic" rate constants of the intermediates in kinetic processes involving back reactions between the intermediates. In the latter case, additional parameters (e.g., equilibrium constants) are needed to describe the reaction. For a unidirectional sequential reaction, the values of the apparent rate constants are the same as those of the intrinsic rate constants, and from eq 1, the elements of the $\mathbf{K}$ matrix are given by

$$K_{ij} = \begin{cases} \dfrac{\prod_{h=1}^{i-1} k_h}{\prod_{h\neq j;\,h=1;i}(k_h - k_j)} & (1 \le j \le i \le N+1) \\ 0 & (1 \le i < j \le N+1) \end{cases} \tag{3}$$

For a photoreaction in which the intermediates are spectrally distinguishable, the time evolution of the reaction can be monitored by the spectral changes after the reaction is initiated by photolysis. We restrict the following discussion to a unimolecular photoreaction monitored by the absorption changes of the sample, which can be expressed as

$$\Delta\mathrm{OD}(\lambda_i, t_j) = \sum_{k=1}^{N+1}(\epsilon_k(\lambda_i) - \epsilon_0(\lambda_i))C_k(t_j) \tag{4}$$

Here $\Delta\mathrm{OD}(\lambda_i,t_j)$ is the difference of the optical densities between the photolyzed and unphotolyzed species monitored at wavelength λ_i and time t_j after photolysis in a unit path length; $\epsilon_k(\lambda_i)$, $\epsilon_{N+1}(\lambda_i)$, and $\epsilon_0(\lambda_i)$ are the extinction coefficients of the kth intermediate, the final product, and the unphotolyzed species at λ_i, respectively, and $C_k(t_j)$ is the concentration of kth intermediate at time t_j. For transient spectroscopic measurements collected at m wavelengths and n delay times after photolysis, eq 4 can be conveniently expressed in matrix form using eq 2

$$\mathbf{A}(\lambda,t) = \epsilon(\lambda)\mathbf{C}(t) = C_0\epsilon(\lambda)\mathbf{K}\mathbf{T}(t) \tag{5}$$

Here $\mathbf{A}$ is an $m \times n$ matrix containing all the *difference* absorption spectra measured at different times following photolysis, and ϵ is an $m \times (N + 1)$ matrix containing the *difference* extinction coefficients of the intermediates and the final reaction product relative to the unphotolyzed species. Our purpose is to extract the spectra (ϵ) and decay rate constants (in $\mathbf{T}$) of the intermediates, together with the reaction mechanism ($\mathbf{K}$), from the raw kinetic data ($\mathbf{A}$).

By defining the matrix of "b-spectra" as

$$\mathbf{B} = C_0\epsilon(\lambda)\mathbf{K} \tag{6}$$

we can decompose the kinetic data into spectral and temporal parts:

$$\mathbf{A}(\lambda,t) = \mathbf{B}(\lambda)\mathbf{T}(t) \tag{7}$$

in which $\mathbf{B}$ is an $m \times (N + 1)$ matrix associated with the observed spectral changes and $\mathbf{T}$ is an $(N + 1) \times n$ matrix containing the apparent rate constants. Equation 7 indicates that the absorption spectrum of the sample at any time, t, after photolysis can be calculated from the linear combinations of the N b-spectra (the concentration of the final product, $C_{N+1} = C_0 - \sum_{i=1}^{N} C_i$, is not an independent variable). Thus the data matrix, $\mathbf{A}$, is of rank N. The most common approach to solve eq 7 is to find the least-square fit for

$$\|\mathbf{R}\| = \|\mathbf{A} - \mathbf{B}\mathbf{T}\| = \sum_{i,j}[\Delta\mathrm{OD}(\lambda_i,t_j) - \sum_{m=1}^{N+1} b_m(\lambda_i)\exp(-k_m t_j)]^2 \tag{8}$$

in which matrix $\mathbf{R}$ ($m \times n$), the difference between the raw data and the fit results, is called the residual spectra.

It is obvious from eq 6 that the b-spectra depend not only on the difference spectra between the intermediates and the unphotolyzed species but also on the mechanism of the reaction, i.e., the way in which the intermediates are interconnected. Therefore, resolution of the reaction mechanism from the transient spectroscopic data involves two steps.

First, the raw kinetic data are fit to eq 7 to determine the number of kinetic intermediates in the reaction, the values of the observed (or apparent) rate constants, and the *b*-spectra associated with these intermediates. Second, the true rate constants and the spectra of the intermediates are constructed from the apparent rate constants and *b*-spectra by assuming a kinetic model from which the **K** matrix can be determined. The difference spectra between the intermediates and the unphotolyzed species can then be calculated from eq 6.

$$\epsilon(\lambda) = \frac{1}{C_0}\mathbf{B}\mathbf{K}^{-1} \tag{9}$$

where the matrix $\mathbf{K}^{-1}$ is the inverse of **K**.

A straightforward fit of eq 8 could be a formidable task, even for a modern supercomputer, since it involves a nonlinear least-square fit of N rate constants and $m \times (N + 1)$ elements in the *b*-spectra. In the present study on phytochrome, for example, the number of nonlinear parameters to be fitted for the *b*-spectra is on the order of $400 \times 5 = 2000$. Fortunately, this difficulty is greatly reduced by the use of singular value decomposition (SVD). The principle of SVD has been described in detail elsewhere.[37,42] The application of SVD to the global analysis of the transient spectral data has helped to resolve the kinetic processes in the photoreactions of other biological pigments such as rhodopsin,[43] bacteriorhodopsin,[41] and hemoglobin.[44]

Briefly, SVD is a powerful computational tool which decomposes any real $m \times n$ matrix ($m \geq n$), **A**, into a set of matrices:

$$\mathbf{A} = \mathbf{U}\mathbf{S}\mathbf{V}^{\mathrm{T}} \tag{10}$$

where **U** ($m \times n$) and **V** ($n \times n$) are orthogonal matrices containing n orthonormal eigenvectors of $\mathbf{A}\mathbf{A}^{\mathrm{T}}$ and $\mathbf{A}^{\mathrm{T}}\mathbf{A}$, respectively, arranged in the sequence of decreasing eigenvalues, and **S** ($n \times n$) is a diagonal matrix whose diagonal elements are the square roots of the eigenvalues of $\mathbf{A}^{\mathrm{T}}\mathbf{A}$. The diagonal elements of **S** ($s_1, s_2, ..., s_n$) are called singular values, where $s_1 > s_2 > ... > s_n \geq 0$. Since matrices $\mathbf{A}^{\mathrm{T}}\mathbf{A}$ and **A** have the same rank, if matrix **A** consists of only k (out of n) independent vectors, then in principle $s_{k+1} = s_{k+2} = s_n = 0$. Therefore, matrix **A** can be represented by a set of reduced orthogonal matrices; only the first k columns of **U** and **V** and first k diagonal elements of **S** are needed to construct **A** in eq 10.

The application of SVD to the kinetics data described by eq 7 will decompose the data matrix, **A**, according to eq 10. For a kinetic reaction involving N intermediates with distinct absorption spectra, only the first N singular values of the data are of significance, while the rest (i.e., s_i with $i > N$) are only of the magnitude of random noise and can be neglected. Therefore, in principle, the kinetic data can be represented by the reduced matrices containing the first N columns of **U** and **V** and the first N singular values. Furthermore, since both **U** and **V** are orthogonal matrices, $\mathbf{U}^{\mathrm{T}}\mathbf{U} = \mathbf{V}^{\mathrm{T}}\mathbf{V} = \mathbf{I}$, where **I** is the identity matrix, and $\|\mathbf{U}^{\mathrm{T}}\mathbf{R}\| = \|\mathbf{R}\|$. Thus the least-square fitting of eq 8 can be simplified by using eq 10 as

$$\|\mathbf{A} - \mathbf{B}\mathbf{T}\| = \|\mathbf{U}(\mathbf{S}\mathbf{V}^{\mathrm{T}} - \mathbf{U}^{\mathrm{T}}\mathbf{B}\mathbf{T})\| = \|\mathbf{S}\mathbf{V}^{\mathrm{T}} - \mathbf{U}^{\mathrm{T}}\mathbf{B}\mathbf{T}\| = \|\mathbf{S}\|\,\|\mathbf{V}^{\mathrm{T}} - \mathbf{S}^{-1}\mathbf{U}^{\mathrm{T}}\mathbf{B}\mathbf{T}\|$$

The above equation indicates that the least-square problem in eq 8 is equivalent to finding the least-square solution for

$$\mathbf{V}^{\mathrm{T}} = \mathbf{D}\mathbf{T} \tag{11}$$

in which matrix $\mathbf{D} = \mathbf{S}^{-1}\mathbf{U}^{\mathrm{T}}\mathbf{B}$.

Therefore, there are several advantages of applying SVD to the analysis of the kinetic data. First, instead of fitting eq 8 which involves a large number of parameters in the *b*-spectra, the nonlinear parameters (i.e., the apparent rate constants) associated with the temporal part of the data can now be fit separately according to eq 11. Second, the dimensions of the matrices for the least-square fitting described by eq 11 can be significantly reduced. Now in eq 11, **V** is an $n \times o$ ($o \geq N$) matrix containing the first o columns of the same matrix in eq 7, **D** is an $o \times (N + 1)$ matrix, and **T** is the $(N + 1) \times n$ matrix containing the apparent rate constants shown in eq 2. As a result, the number of parameters to be fit is reduced to the N apparent rate constants and the number of elements of the **D** matrix, which is only about 50 in the current study on phytochrome. Therefore, SVD provides an efficient approach to reduce the dimensions of the matrices and the number of parameters for global fitting. In practice, the value of o is chosen to be slightly larger than N. The convergence of the fitting is reached when the value of the total residual, $(\|\mathbf{R}\|)^{1/2}$, is smaller than a numerical limit. The quality of the fitting is measured by the residual spectra, **R**. For a proper fit (e.g., with an appropriate number of intermediates), the residual spectra at different times and different wavelengths should only consist of random noise without spectral features. The *b*-spectra can be calculated from the results of the global fitting of eq 11:

$$\mathbf{B} = \mathbf{U}\mathbf{S}\mathbf{D} \tag{12}$$

Note that the random noise in the *b*-spectra is dramatically reduced by using SVD since only the reduced forms of the matrices **U** ($m \times o$) and **S** ($o \times o$) are used in the above calculation.

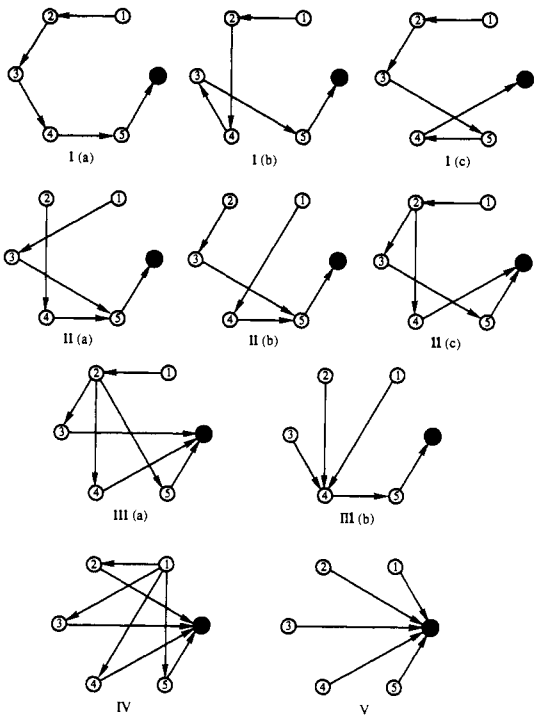

Figure 2. Examples of simple kinetic schemes of a unimolecular reaction with five metastable intermediates (the open circles) and the final reaction product (the solid circle). Each intermediate is associated with an apparent rate constant and is labeled by a number. For the convenience of discussion, the apparent rate constants are arranged such that $k_1 > k_2 > k_3 > k_4 > k_5$. The unidirectional sequential reactions shown in scheme I a,b,c can be represented as (k_1, k_2, k_3, k_4, k_5), (k_1, k_2, k_4, k_3, k_5), and (k_1, k_2, k_3, k_5, k_4), respectively. Schemes II–V represent the kinetic models with two, three, four, and five parallel pathways, respectively. For the sake of simplicity, back reactions and cross reactions are not considered.

Criteria for Kinetic Models

It is important to realize that the global fitting procedure using SVD only extracts the information of the apparent variables (i.e., the apparent rate constants and the *b*-spectra) from the raw experimental data and is independent of any specific kinetic models. In fact, the absorption spectra of the intermediates calculated from assuming a particular kinetic model are often used as a criterion to judge whether the model is realistic. To study all possible kinetic models comprehensively could be a challenging task for a moderately complicated reaction. As an example, Figure 2 illustrates a few types of possible models involving five intermediates. Here each open circle represents an intermediate associated with a *b*-spectrum and an apparent rate constant. The intermediate labeled with a number i means it decays with the apparent rate constant of k_i. For simplicity, back reactions are not included in these cases, and the apparent rate constants are defined in a decreasing order (i.e., $k_i > k_j$ for $i < j$). The solid circle represents the final reaction product. A kinetic model is simply a specific pattern of the interconnections among the intermediates and the reaction product and can be represented by

(42) Forsythe, G. E.; Malcolm, M. A.; Moler, C. B. *Computer Methods for Mathematical Computations*; Prentice-Hall: Englewood Cliffs, NJ, 1977.
(43) Hug, S. J.; Lewis, J. W.; Einterz, C. M.; Thorgeirsson, T. E.; Kliger, D. S. *Biochemistry* **1990**, *29*, 1475–1485.
(44) Hofrichter, J.; Henry, E. R.; Sommer, J. H.; Deutsch, R.; Ikeda-Saito, M.; Yonetani, T.; Eaton, W. A. *Biochemistry* **1985**, *24*, 2667–2679.

a unique **K** matrix for each pattern. Scheme I in Figure 2 illustrates the examples of unidirectional sequential models, and schemes II–V illustrate the models with an increasing number of parallel pathways. Even for scheme I, the simplest case, there are a total of 5! = 120 possible models. Fortunately, it is often possible to preclude many possibilities if the apparent rate constants and the absorption spectra of the intermediates differ significantly from each other. In this case the models that seem to disagree with the general features of the kinetic data will usually generate spectra that do not satisfy the criteria to be discussed below.

The validity of a given kinetic model is commonly judged by the following criteria regarding the absorption spectra and the true rate constants calculated from the model (see ref 41 for a more complete discussion). First, the absorbance of each intermediate should be positive at any wavelength. Second, the absorption spectra should be a smooth function of the wavelength and, for a particular absorption band of a chromophore, should consist of only one main absorption maximum. Furthermore, the absorption spectra of the kinetic intermediates obtained from a realistic model should be able to explain the absorption spectra obtained from the low-temperature steady-state studies. However, caution should be taken when comparing the absorption spectra of the intermediates at physiological temperatures and those obtained at low temperatures. This is not only because the absorption maximum and the extinction coefficient of an intermediate could change with the temperature but also because the steady-state absorption spectrum at a certain temperature does not necessarily represent the spectrum of a single intermediate (especially when the intermediates decay in parallel pathways) and can often be interpreted by more than one kinetic model, as will be discussed more explicitly below for the case of the phytochrome phototransformation. More importantly, the path(s) of the reaction is determined by the surface of the free energy ($G = H - TS$, in which H and S are the enthalpy and and entropy of the system, respectively) and therefore could be strongly temperature dependent.

Generally, the trapping of an intermediate at low temperature can take place either because there are high potential barriers between the intermediate and the nearby metastable states or because the intermediate is lowest in free energy relative to the other local potential minima at that temperature. In the latter case, the equilibrium between the trapped intermediate and the next intermediate should be observed as the temperature is raised to their transition temperature, at which $\Delta G(T) = 0$. Here we may assume that the enthalpies (H) of the intermediates are not strongly temperature dependent in a narrow temperature range, so that the change in the relative free energy (ΔG) with temperature is chiefly due to the entropy terms ($T\Delta S$). For an "entropy-driven" process ($\Delta S > 0$), i.e., the free energy of the second intermediate decreases faster than that of the first intermediate as the temperature increases, if a kinetic equilibrium between two intermediates is observed by time-resolved studies at high (e.g., physiological) temperatures, then it is impossible to trap the second intermediate as a stable species at lower temperatures. This is due to the fact that the free energy of the second intermediate relative to the first intermediate will increase as the temperature decreases, which will make the second intermediate energetically unfavorable ($\Delta G(T) > 0$) at the lower temperatures. Therefore, it is possible to observe more intermediates in time-resolved studies at higher temperatures than in low-temperature steady-state studies. This has been observed in the photoreaction of bovine rhodopsin[43] and will be explained in more detail in the discussion of transient circular dichroism studies of phytochrome intermediates.[45] Despite the fact that the reaction mechanism could be temperature dependent, the intermediates trapped at low temperatures have been observed to be similar to those at physiological temperatures in various biological pigments. Therefore, we think that the consistency between the results of low-temperature steady-state measurements and time-resolved measurements at physiological temperatures is a valid criterion for the phytochrome phototransformation.

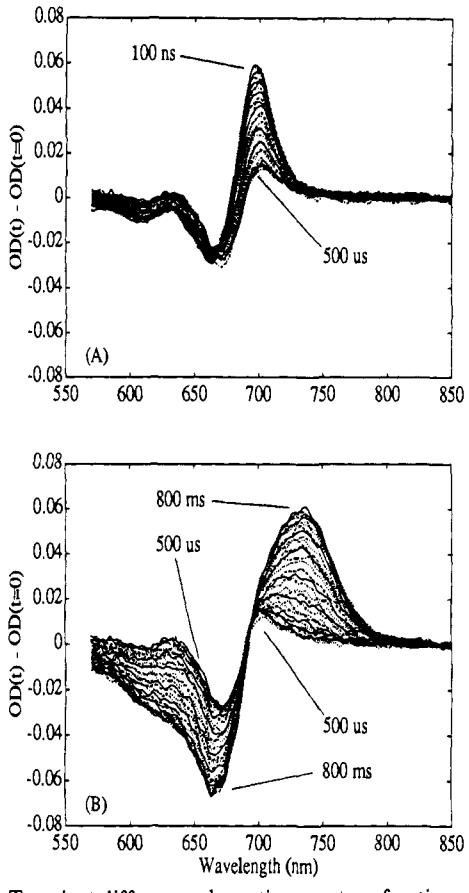

Figure 3. Transient difference absorption spectra of native oat phytochrome at 10 °C. The spectra were collected at logarithmic delay times from 100 ns to 800 ms following 7-ns laser photolysis, with 10 points in each time decade. Each spectrum represents the average of 32 single photolysis measurements smoothed by a 15-point Savitzky-Golay algorithm. (A) Transient difference spectra from 100 ns to 500 μs. (B) Transient difference spectra from 500 μs to 800 ms.

Additional criteria come from the measurements of the temperature dependence of the kinetic data. In a small temperature range, the absorption spectra of the intermediates should not be strongly temperature dependent, and the temperature dependence of the true (not apparent) rate constants should lead to linear Arrhenius plots. The first criterion seems to be valid for phytochrome since the changes of the absorption spectra of Pr and Pfr are relatively small between 0 and 30 °C.[46] In this study, we consider first the unidirectional models for the sake of simplicity. Back reactions between the intermediates are considered only when it appears necessary.

Results

The transient difference absorption spectra of the forward phototransformation of native oat phytochrome are shown in Figure 3. The data represent 65 difference spectra, which were collected at 10 °C from 100 ns to 800 ms after photolysis. Each spectrum contains approximately 480 wavelength points. The difference spectrum at each time is the average of two sets of 16 single photolysis measurements, smoothed by a 15-point Savitzky–Golay algorithm.[47] The base lines of all the spectra were corrected by assuming that the transient difference absorbances between 830 and 850 nm were zero. The time-resolved absorption data indicate that the phototransformation can be divided into

(45) Björling, S. C.; Zhang, C.-F.; Farrens, D.; Song, P.-S.; Kliger, D. S. *J. Am. Chem. Soc.*, following article in this issue.

(46) Sasaki, N.; Oji, Y.; Yoshizawa, T.; Yamamoto, K. T.; Furuya, M. *Photochem. Photobiophys.* **1986**, *12*, 243–251.

(47) Savitzky, A.; Golay, M. J. E. *Anal. Chem.* **1964**, *36*, 1627–1639.

early and late stages, as shown in Figure 3A,B, respectively. By comparing the transient difference spectra with the absorption spectra of the intermediates obtained by a low-temperature steady-state study,[18] the following rough scheme can be seen from our data: a lumi-R intermediate(s) is formed immediately after the photolysis and is transformed to the meta-Ra intermediate(s) within 100 μs, as shown by the decrease of the absorbance at 690 nm on this time scale (Figure 3A); the formation of meta-Rc and possibly Pfr from the meta-Ra intermediate(s) is observed after 10 ms, as indicated by the increase of absorbance at 730 nm and bleaching at 660 nm at these times (Figure 3B). The last dark reaction was not completed by 800 ms, as the difference spectrum at 20 s after photolysis exhibited a larger absorbance at 730 nm and the same bleaching at 660 nm compared to that at 800 ms (data not shown). In order to obtain a quantitative analysis of the phototransformation data, we performed global analysis of all of the transient absorption spectra simultaneously according to the method explained in the previous section.

Global Fitting of Time-Resolved Absorption Spectra. The first part of the global analysis was to determine the number of intermediates, the apparent rate constants, and the *b*-spectra. This was carried out in two steps. First, the transient absorption data of Pr were analyzed by SVD, which indicated that the diagonal elements of the S matrix were 3.10, 1.21, 0.472, 0.091, 0.038, 0.032, ..., 0.0027 (65 singular values in total). The significant relative magnitudes of the first three singular values imply that at least three spectrally independent intermediates are present in the phototransformation from Pr to Pfr. Second, the temporal part of the data (i.e., the reduced form of matrix V) obtained from the SVD analysis was fit according to eq 11 by using a Simplex algorithm. Comparisons were made for the residual spectra obtained from the global fits assuming different numbers of intermediates (≥3) in the phototransformation. The results of the global fitting were not sensitive to the size of the reduced matrix V as long as the number of columns in matrix V (i.e., *o*) was larger than the number of intermediates. For the results presented in this paper, $o = 10$. The fact that the residual spectra for a proper fitting should only comprise random noise was used as the main criterion to determine the number of kinetic processes in the phototransformation. If the transient data were fit assuming three rate constants, the lifetime of the first intermediate was found to be roughly 40 μs. It was evident that structural features representing nonrandom noise (>5% of the difference OD spectra) could be seen in certain residual spectra at the early times (100 ns–100 μs, results not shown). The quality of the fitting was dramatically improved by assuming the existence of an additional intermediate. This implies that the transient data cannot be sufficiently described by three kinetic processes and that the phototransformation from Pr to Pfr involves at least four intermediates. In this case, the apparent lifetimes of the intermediates were 7.1 μs, 84.9 μs, 10.7 ms, and 93.8 ms. As will be discussed in detail later, the detection of a fast decay process with a 7-μs lifetime was well within the time resolution of our measurements.

The fact that the residual spectra at the early times are primarily comprised of random noise indicates that our data can be fit rather satisfactorily with four kinetic processes. However, it was found that the total residual, $(\|\mathbf{R}\|)^{1/2}$ was reduced by 5% when the global fitting was carried out for five intermediates. Although this improvement was close to the noise level in our data, it was still observable that the residual spectra around 730 nm were improved in the late times (>100 ms). Furthermore, the apparent rate constant and the *b*-spectrum of the fifth intermediate were reproduced consistently in the different sets of experimental data. The small improvement of the total residual found in the fitting by assuming the additional intermediate in the phototransformation was probably due in part to the fact that measurements were not taken at sufficiently long delay times (i.e., seconds) due to experimental limitations. Our measurements at much longer times (~20 s) indicated that the formation of Pfr was not completed by 800 ms, which confirmed that the decay time of the last step of the phototransformation should be considerably longer than that of the last intermediate (94 ms) obtained

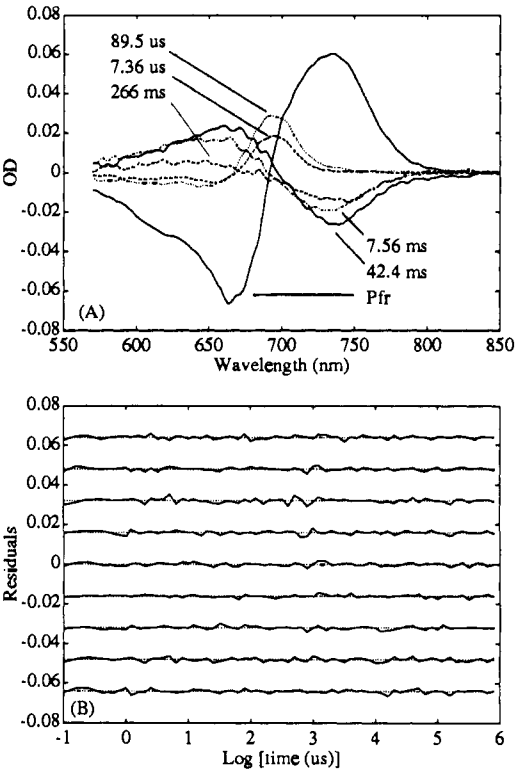

Figure 4. Results of global analysis ($N = 5$) of the transient difference data shown in Figure 3. (A) B-spectra calculated from the global analysis assuming five intermediates. Each *b*-spectrum is associated with an apparent rate constant as labeled. The last *b*-spectrum represents the difference spectrum between Pfr and Pr. (B) Residual spectra (versus the logarithm of time) at a few select wavelengths; from top to bottom: 600, 630, 660, 690, 710, 730, 750, 780, and 800 nm. The small spikes at certain time points are probably due to the base line drifts in the spectral measurements at those times.

from the global fitting assuming four intermediates. The attempt to fit the transient data by assuming the presence of a sixth intermediate led to divergence. These results combine to suggest that the forward phototransformation from Pr to Pfr should involve five kinetic intermediates. The apparent lifetimes associated with these intermediates are 7.36 μs, 89.5 μs, 7.56 ms, 42.4 ms, and 266 ms. The last decay time constant could be considerably underestimated due to the lack of measurements at sufficiently long decay times (i.e., seconds) after photolysis. In fact, the time constant of the slowest kinetic process obtained from different sets of experiments was found to have a large error (up to 50%). The *b*-spectra associated with these kinetic processes and the residuals at a few select wavelengths are shown in Figure 4A,B, respectively. The *b*-spectrum associated with the slowest decay process was not sensitive to the variation of the value of the apparent time constant.

Testing Kinetic Models. The second part of the analysis involves the testing of different kinetic models from which the true rate constants and the absorption spectra of the intermediates are calculated. The absorption spectra of the intermediates were obtained by the estimation that 15% of Pr was photolyzed in the actinic volume. Both the value of the photolysis yield and the absorption spectrum of Pfr generated from the difference spectrum by assuming this yield are in good agreement with previous results in the literature. The value of 15% photolysis yield was used in all the later studies to calculate the absorption spectra of the intermediates and Pfr. Since the phototransformation of phytochrome is a rather complicated reaction involving five intermediates, it is nearly impossible to examine all of the possibilities represented in Figure 2. However, the fact that the intermediates of the phytochrome phototransformation have distinct absorption spectra and dramatically different decay rate constants significantly simplifies the analysis and makes it possible to exclude many possiblities before any serious consideration of plausible models.

For the sake of convenience in the following discussions, the apparent rate constants are defined in such a way that $k_1 > k_2 > k_3 > k_4 > k_5$.

As we noted earlier, even for a simple unbranched unidirectional reaction, scheme I in Figure 2 corresponds to 5! = 120 possible kinetic models. However, it can be easily shown that the only realistic model is (k_1, k_2, k_3, k_4, k_5). Other patterns of interconnections, such as (k_2, k_1, k_3, k_4, k_5), (k_1, k_2, k_4, k_3, k_5), or (k_1, k_2, k_3, k_5, k_4), can be simply ruled out since the absorption spectra of the intermediates derived from these models (see more discussion below for the calculations of the absorption spectra from the difference spectra of the intermediates) contain large negative absorption bands and therefore do not satisfy the criteria for a realistic model discussed previously. Consequently, we can conclude that for any realistic model of phytochrome phototransformation, the sequential part of the reaction (or reaction branches) must proceed with monotonically decreasing rate constants. This is rather obvious for the phytochrome phototransformation since the apparent rate constants of the kinetic processes differ significantly from each other.

It can be seen from the apparent lifetimes obtained from the global analysis that the phototransformation from Pr to Pfr proceeds in two stages: the fast reactions (k_1 and k_2) which are completed in the microsecond regime and the slow reactions (k_3, k_4, and k_5) in the millisecond time regime. It is usually easier to study a reaction mechanism in a "bottom-up" fashion (i.e., from the late stage to the early stage of the reaction) since the difference absorption spectrum between the final product (Pfr) and the unphotolyzed species (Pr) is known. On the basis of the fact that the absorbance increase near 730 nm is observed only after 10 ms, the possibilities of more than three parallel pathways leading to Pfr (i.e., schemes IV and V in Figure 2) can be excluded considering the rate constants obtained from the global analysis. In fact, the absorption spectra derived from these models were again found to exhibit negative absorbance in certain spectral regions. The model with three parallel pathways to Pfr, such as that illustrated in scheme III a, can also be ruled out since the absorption spectrum of the slowest intermediate (meta-Rc) deconvoluted from this model exhibits two peaks rather than one (results not shown). The model shown in scheme III b was found to exhibit abnormally large absorption spectra for the early intermediates (i.e., lumi-R) compared to that of Pr and Pfr and thus should not be considered as a plausible candidate. Similar examinations of the other models lead to the conclusion that there should not be more than two parallel pathways in the phytochrome phototransformation.

As a result of these observations, only the unique sequential reaction (k_1, k_2, k_3, k_4, k_5) in scheme I and a few models with two parallel pathways shown in scheme II warrant further consideration. An additional restriction comes from the examination of scheme II c in which the final product, Pfr, is formed from two parallel pathways. The absorption spectra of the intermediates appeared to be positive in the spectral region when it was assumed that the first intermediate (lumi-R) decayed into the two parallel pathways with equal rate constants (i.e., $k_1/2$, results not shown). However, the slowest intermediate, which was the only intermediate with the spectral shape similar to that of meta-Rc, exhibited dramatically reduced absorption compared to the spectrum of meta-Rc at low temperatures.[18] Although the lack of agreement with the low-temperature results could not be used to simply rule out this model, the models with parallel pathways leading to Pfr seem less plausible compared to the other models to be discussed below. Therefore, it is likely that the formation of Pfr proceeds from a single intermediate (meta-Rc). Since the decay from meta-Rc to Pfr (>266 ms) is significantly slower than the other processes, the absorption spectrum of meta-Rc can be approximately determined irrespective of the mechanisms of the previous dark reactions. It was found that the absorption spectrum of meta-Rc was similar to that of Pfr with a slightly reduced extinction coefficient near 730 nm (refer to Figures 6 and 7 for more detail). Therefore a realistic model cannot have more than two parallel pathways leading to meta-Rc for the reasons mentioned previously. The formation of meta-Rc must proceed from the slow intermediate(s) in the late stage of the phototransformation.

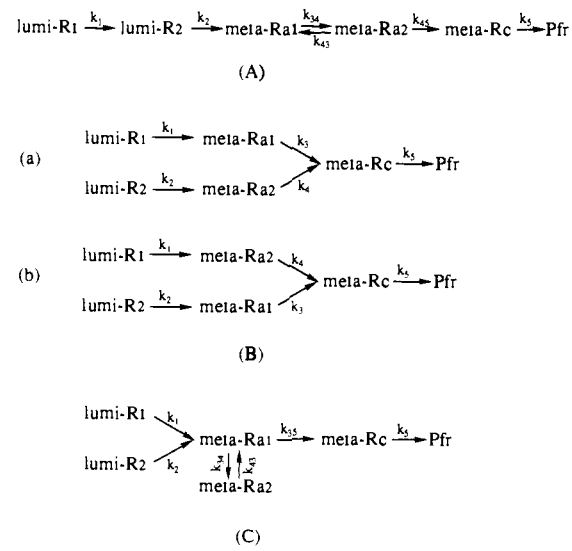

Figure 5. Plausible kinetic models for the phototransformation of native oat phytochrome. The intermediates, lumi-R1, lumi-R2, meta-Ra1, meta-Ra2, and meta-Rc, are associated with the first five *b*-spectra shown in Figure 3B, with their apparent rate constants in a decreasing order. (A) A simple sequential model with one back reaction required to yield a normal absorption spectrum of meta-Ra2. (B) Models with two parallel pathways. The slowest dark reaction, i.e., from meta-Rc to Pfr, is still a sequential process. (C) A model between A and B. The early intermediates decay in a parallel pathway, but the latter intermediates decay in a sequential pathway. Also notice that the equilibrium between meta-Ra1 and meta-Ra2 is different from that shown in A.

We now consider a limited number of simple models with the five intermediates designated as lumi-R1, lumi-R2, meta-Ra1, meta-Ra2, and meta-Rc. This nomenclature of the intermediates is partly derived from the similar spectral properties between these intermediates and the low-temperature intermediates.[18] The models which meet the conditions described above are shown in Figure 5.

(I.) Unbranched Sequential Models. The difference spectra between the intermediates (including Pfr) and Pr derived from the simple sequential model (scheme I in Figure 2) were calculated from eq 12. The difference spectra and the absorption spectra of the intermediates obtained by adding 15% of the absorption spectrum of the unphotolyzed species (Pr) to the difference spectra are shown in Figure 6A,B, respectively. It is evident from Figure 6B that the absorption spectrum of meta-Ra2 obtained from this unidirectional sequential model exhibits two broad bands, with one near the absorption maxima of meta-Ra1. This suggests that there is an equilibrium between the meta-Ra1 and meta-Ra2 intermediates.

It is rather complicated to formulate the **K** matrix for six species (including Pfr as the final product of the phototransformation) with back reactions between different intermediates. Fortunately, this problem can be resolved technically by treating the early and late stages of the phototransformation as two separate, smaller reactions, i.e., lumi-R1 → lumi-R2 → meta-Ra1 and meta-Ra1 ↔ meta-Ra2 → meta-Rc → Pfr. This approach is appropriate because the formation of meta-Ra1 from lumi-R2 (~80 μs) is so much more rapid than the decay of meta-Ra1 to meta-Ra2 (~7 ms) that meta-Ra1 in the second reaction can be regarded as a "stable" initial intermediate formed instantaneously from the first reaction. The errors to the rate constants and the absorption spectra of the intermediates in making this approximation should be on the order of $k_3/k_2 \approx 1\%$, which is within the noise level of our data. The **K** matrices of the two subreactions are as given in Chart I, where k_{34} and k_{43} are the rate constants of the forward and back reactions between meta-Ra1 and meta-Ra2, respectively, and k_{45} is the true rate constant for the decay of meta-Ra2 to meta-Rc. The formulas for the true rate constants are the same as that for a simpler case described by Bamford and Tipper.[48] The

Chart I

$$\mathbf{K}_1 = \begin{pmatrix} 1 & 0 & 0 \\ k_1/(k_2-k_1) & k_1/(k_1-k_2) & 0 \\ -k_2/(k_2-k_1) & -k_1/(k_1-k_2) & 1 \end{pmatrix}$$

$$\mathbf{K}_2 = \begin{pmatrix} (k_4-k_{34})/(k_4-k_3) & (k_3-k_{34})/(k_3-k_4) & 0 & 0 \\ k_{34}/(k_4-k_3) & k_{34}/(k_3-k_4) & 0 & 0 \\ k_{34}k_{45}/(k_4-k_3)(k_5-k_3) & k_{34}k_{45}/(k_3-k_4)(k_5-k_4) & k_{34}k_{45}/(k_3-k_5)(k_4-k_5) & 0 \\ -k_{34}k_{45}k_5/k_3(k_4-k_3)(k_5-k_3) & -k_{34}k_{45}k_5/k_4(k_3-k_4)(k_5-k_4) & -k_{34}k_{45}/(k_3-k_5)(k_4-k_5) & 1 \end{pmatrix}$$

Chart II

$$\mathbf{K}_1 = \begin{pmatrix} 1 & 0 & 0 & 0 & 0 & 0 \\ 0 & 0 & 0 & 0 & 0 & 0 \\ k_1/(k_3-k_1) & 0 & k_1/(k_1-k_3) & 0 & 0 & 0 \\ 0 & 0 & 0 & 0 & 0 & 0 \\ k_1k_3/(k_3-k_1)(k_5-k_1) & 0 & k_1k_3/(k_1-k_3)(k_5-k_3) & 0 & k_1k_3/(k_1-k_5)(k_3-k_5) & 0 \\ -k_3k_5/(k_3-k_1)(k_5-k_1) & 0 & -k_1k_5/(k_1-k_3)(k_5-k_3) & 0 & -k_1k_3/(k_1-k_5)(k_3-k_5) & 1 \end{pmatrix}$$

$$\mathbf{K}_2 = \begin{pmatrix} 0 & 0 & 0 & 0 & 0 & 0 \\ 0 & 1 & 0 & 0 & 0 & 0 \\ 0 & 0 & 0 & 0 & 0 & 0 \\ 0 & k_2/(k_4-k_2) & 0 & k_2/(k_2-k_4) & 0 & 0 \\ 0 & k_2k_4/(k_4-k_2)(k_5-k_2) & 0 & k_2k_4/(k_2-k_4)(k_5-k_4) & k_2k_4/(k_2-k_5)(k_4-k_5) & 0 \\ 0 & -k_4k_5/(k_4-k_2)(k_5-k_2) & 0 & -k_2k_5/(k_2-k_4)(k_5-k_4) & -k_2k_4/(k_2-k_5)(k_4-k_5) & 1 \end{pmatrix}$$

absorption spectrum of meta-Ra2 showed a single positive band only when the equilibrium constant, K_{eq} (k_{34}/k_{43}), was set to be approximately 1.5. The absorption spectra of the transient intermediates derived from this reaction scheme (Figure 5A) are shown in Figure 7A. In fact, the designation of the "meta-Ra2" may not be so appropriate in this case since the absorption spectrum of this intermediate actually resembles that of meta-Rc. The time constants of the forward and back reactions ($1/k_{34}$ and $1/k_{43}$) and that from meta-Ra2 to meta-Rc ($1/k_{45}$) are 15.5, 23.3, and 20.7 ms, respectively. The rate constants for the rest of the reactions, i.e., k_1, k_2, and k_5, are the same as the apparent rate constants.

(II.) Parallel Models with Two Branches. The two possible simple models involving two parallel pathways to form meta-Rc are shown in Figure 5B. These models correspond to scheme II a and b in Figure 2. The **K** matrix for the reaction model shown in Figure 5B a can be expressed as $\mathbf{K} = a\mathbf{K}_1 + (1-a)\mathbf{K}_2$, where a is the fraction of the phototransformation proceeding by the upper branch in Figure 5B a and $\mathbf{K}_1$ and $\mathbf{K}_2$ are the matrices for the two sequential reaction branches (Chart II).

The **K** matrix for model b in Figure 5B can be obtained with a similar approach. The partition constant, a, was adjusted so that the absorption spectra of all the intermediates calculated from eq 12, assuming 15% photolysis yield, have normal profiles and positive absorbance in the spectral region of interest. For the models shown in Figure 5B a and b, the fractions of the phototransformation to the first parallel pathway (i.e, through lumi-R1) were found to be 0.45 and 0.55, respectively. The transient absorption spectra of the intermediates derived from these parallel models are shown in Figure 7B a and b, respectively.

(III.) Other Possibilities. Figure 5C illustrates an interesting alternative first suggested by Eilfeld and co-workers.[34] This model lies somewhere between cases I and II. It assumes parallel decays of the lumi-R intermediates and a sequential formation of meta-Rc from meta-Ra1. It was not included in Figure 2 since it contained an equilibrium between meta-Ra1 and meta-Ra2 aside from the main pathway of the phototransformation and therefore was not considered as a simple model. The early stage (i.e., the decays of the lumi-R intermediates) and the late stage (i.e., the decays of the meta-Ra and meta-Rc intermediates to form Pfr) of the phototransformation were again treated separately. The **K** matrices for the parallel decays of the lumi-R intermediates ($\mathbf{K}_1$) and the sequential decays of the meta-Ra and meta-Rc intermediates

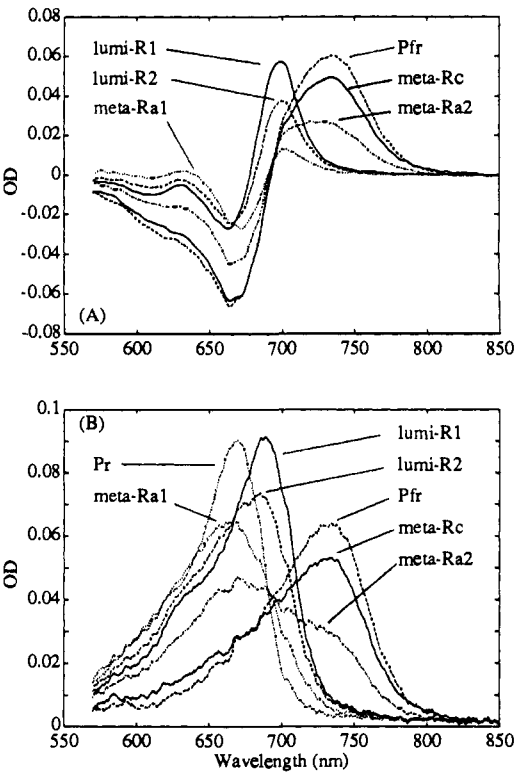

Figure 6. (A) Difference absorption spectra between the intermediates and the unphotolyzed species Pr and (B) their absorption spectra derived from the simple sequential model without back reactions. The absorption spectra of the intermediates were obtained by adding 15% Pr spectra to the difference spectra calculated from global analysis according to eq 12 in the text. The shape of the meta-Ra2 spectrum (B) suggests that meta-Ra1 and meta-Ra2 are in equilibrium.

(48) Bamford, C. H., Tipper, C. F. H., Eds., *Chemical Kinetics, Modern Methods in Kinetics*; Elsevier Scientific Publishing Company: New York, 1969; Vol. 24.

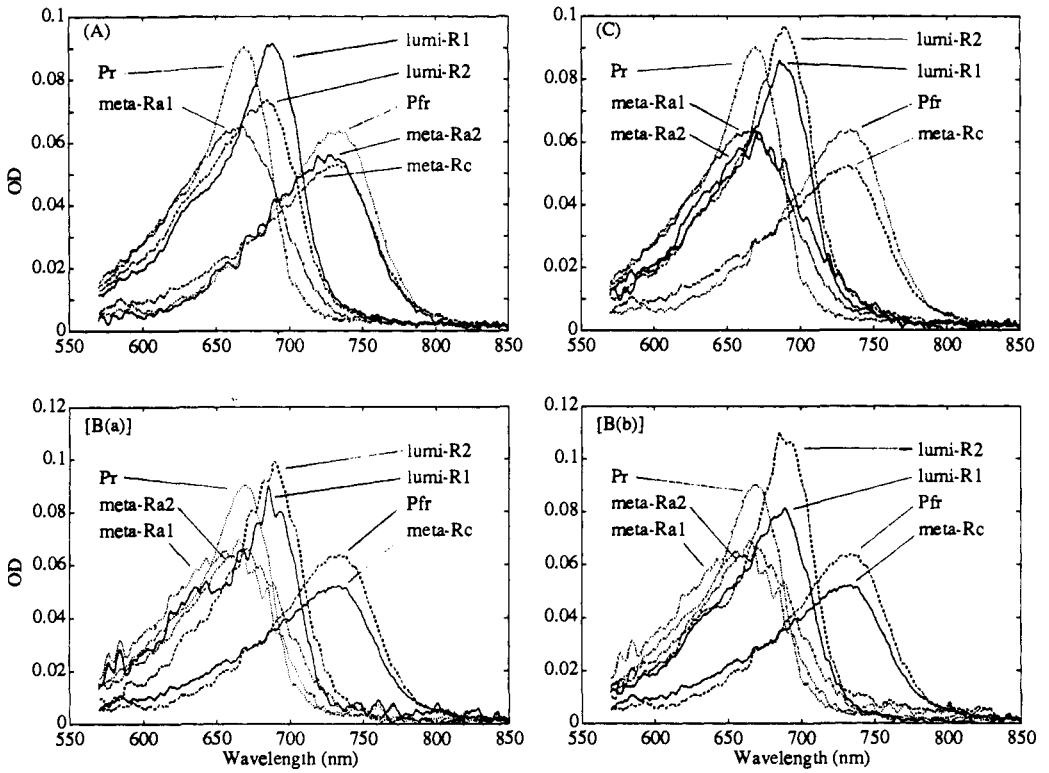

Figure 7. Absorption spectra of the intermediates derived from the models shown in Figure 5. The apparent rate constants k_1, k_2, k_3, k_4, and k_5 are 1.36×10^5, 1.12×10^4, 132.3, 23.6, and 3.76 s^{-1}, respectively. (A) Absorption spectra in a sequential pathway shown in Figure 5A with the equilibrium constant $K_{eq} = k_{34}/k_{43} = 1.5$. The true rate constants of the forward and back reactions (k_{34} and k_{43}) and that from meta-Rc to Pfr (k_{45}) are 64.5, 43.0, and 48.3 s^{-1}, respectively, while the other rate constants, k_1, k_2, and k_5, are identical to the apparent rate constants. The spectrum of meta-Ra2 resembles that of meta-Rc. (B, a and b) Absorption spectra derived from the models with two parallel pathways shown in Figure 5B a and b, respectively. (C) Absorption spectra derived from the model shown in Figure 5C. The equilibrium constant $K_{eq} = k_{34}/k_{43} = 0.85$. The true rate constants, k_{34}, k_{43}, and k_{35}, were found to be 43.8, 51.5, and 60.5 s^{-1}, respectively. The other rate constants, k_1, k_2, and k_5, are identical to the apparent rate constants. The absorption spectrum of meta-Ra2 was found to be very similar to that of meta-Ra1.

Chart III

$$\mathbf{K}_1 = \begin{pmatrix} a & 0 & 0 \\ 0 & 1-a & 0 \\ -a & a-1 & 1 \end{pmatrix}$$

$$\mathbf{K}_2 = \begin{pmatrix} (k_{43}-k_3)/(k_4-k_3) & (k_{43}-k_4)/(k_3-k_4) & 0 & 0 \\ k_{34}/(k_4-k_3) & k_{34}/(k_3-k_4) & 0 & 0 \\ k_{35}(k_{43}-k_3)/(k_4-k_3)(k_5-k_3) & k_{35}(k_{43}-k_4)/(k_3-k_4)(k_5-k_4) & k_{35}(k_{43}-k_5)/(k_3-k_5)(k_4-k_5) & 0 \\ -k_5(k_4-k_{35})/(k_4-k_3)(k_5-k_3) & -k_5(k_3-k_{35})/(k_3-k_4)(k_5-k_4) & -k_{35}(k_{43}-k_5)/(k_3-k_5)(k_4-k_5) & 1 \end{pmatrix}$$

($\mathbf{K}_2$) can be expressed as shown in Chart III, in which a is the fraction of the initial concentration of lumi-R1, k_{34} and k_{43} are the rate constants of the forward and back reactions between meta-Ra1 and meta-Ra2, respectively, and k_{35} is the true rate constant of the meta-Ra1 to meta-Rc reaction. The true rate constants can be calculated from the apparent rate constants (k_3 and k_4) from

$$k_{43} = [k_3 + k_4 + \sqrt{(k_3 - k_4)^2 - 4K_{eq}k_3k_4}]/2(1 + K_{eq})$$

where K_{eq} is the equilibrium constant (k_{34}/k_{43}) and $k_{34} = K_{eq}k_{43}$ and $k_{35} = k_3k_4/k_{43}$. It was found that the best equilibrium constant between the meta-Ra1 and meta-Ra2 intermediates for this model was 0.85. The true time constants, $1/k_{34}$, $1/k_{43}$, and $1/k_{35}$, were found to be 22.8, 19.4, and 16.5 ms, respectively. The absorption spectra of the intermediates derived from this model are shown in Figure 7C.

Absorption Measurements in the UV Region. We were also interested in the spectral changes in the near-UV and blue spectral regions at the different stages of the phototransformation from Pr to Pfr. The transient difference absorption spectra in this region taken at a few select delay times following photolysis are shown in Figure 8A. Due to the fact that a large number of averages were required to obtain good signal/noise ratios for these transient difference spectra, the measurements were taken at only one delay time per time decade. Each difference spectrum in Figure 8A represents the average of two sets of data obtained from 64 and 80 single photolysis measurements, respectively, smoothed by a 15-point Savitzky–Golay algorithm. The transient absorption spectra at these times obtained by adding the 15% Pr spectrum to the difference spectra are shown in Figure 8B.

Discussion

We have shown above how the use of the global analysis of time-resolved absorption spectra yielded the kinetics and the absorption spectra of the intermediates involved with several possible mechanisms of the phototransformation of native oat phytochrome. The reaction mechanisms presented in Figure 5 represent the simplest models consistent with the results of the global analysis of our data and are not a complete list of all the possibilities. For example, the present study did not examine any models with reversions from various intermediates back to Pr and thus assumed a unit photolysis yield for every dark reaction in the phototransformation. In choosing only the simplest mecha-

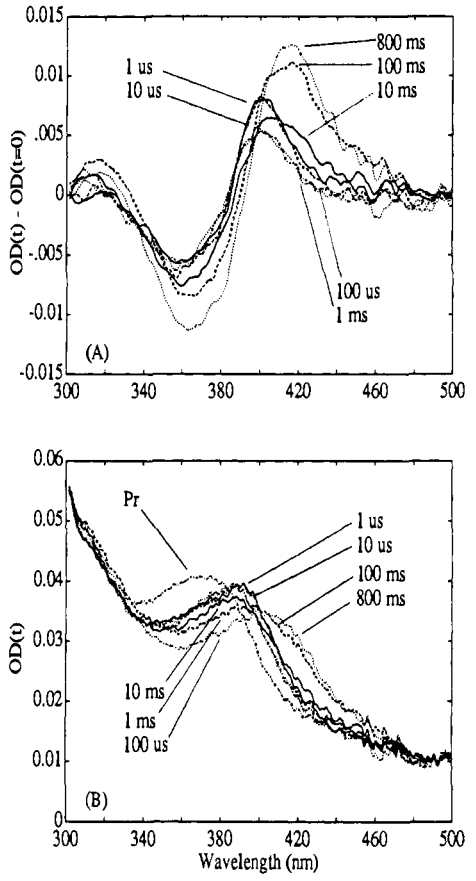

Figure 8. (A) Transient difference absorption spectra and (B) absorption spectra of native oat phytochrome (at 10 °C) in the UV spectral region measured at various delay times after laser photolysis. The absorption spectra were obtained by adding the 15% Pr spectrum to the difference spectra. The transient spectrum at 100 ns is identical to that at 1 μs except for a base line offset and is therefore not shown here. Each difference spectrum represents the average of 144 single photolysis measurements smoothed by a 15-point Savitzky-Golay algorithm.

nisms we employ Occam's razor, which suggests that the simplest mechanism that can explain the data is most appropriate. More complicated mechanisms should be introduced only as new evidence is found that suggests the need for more complex solutions. At present we cannot determine whether the decays of the lumi-R and meta-Ra intermediates proceed by sequential or parallel pathways.

Our results on the early stage of the phototransformation of native oat phytochrome are in good agreement with previous studies.[30,35] We found that the decay times of the first two intermediates were approximately 7.4 and 89.5 μs at 283 K, comparing favorably with the results of Ruzsicska and co-workers who observed that the absorbance at 695 nm decayed with the time constants of 11 and 102 μs at 281 K. They attributed the biexponential decay to the presence of two lumi-R species.[35] Cordonnier et al. also found that, for "undegraded" oat phytochrome at 275 K, the decay of absorbance at 694 nm had to be described by two first-order processes, with time constants of approximately 14.5 and 217 μs.[30] These results can be compared with those presented in this study since the kinetics at the early stage of the phototransformation are not sensitive to different sample conditions.[35] The fast decay of lumi-R was not resolved in a number of recent studies performed at room temperature.[19,26] This was probably due to the fact that the time resolutions in these measurements were not sufficient to resolve the first intermediate, which was found to decay in approximately 3 μs at 298 K.[35]

We verified that the fast decay evident from our data could not be due to potential artifacts such as the use of the relatively large sampling gate (500 ns) in our measurements. If the transient data is fit by assuming only three intermediates in the phototransformation, the lumi-R intermediate is found to decay with a time constant of about 40 μs (instead of 7.4 and 89.5 μs). As we noted earlier in the Results section, this approach would produce poor residual spectra at early times after photolysis, indicating that the fitting of the transient data required more intermediates. This is not due to kinetic artifacts induced by the molecular rotation following linearly polarized photolysis since all the measurements are performed using magic angle detection. Furthermore, the rotational relaxation of the phytochrome dimer is approximately 100 ns at physiological temperature,[49] which is too fast to induce kinetic artifacts in the microsecond regime. In order to investigate whether the 500-ns sampling gate used in our measurements could make the transient data at early times deviate from a single exponential decay, we performed a global analysis on computer-generated data which simulated the "gate effects" on the transient data under conditions similar to those of the experimental data. We found that the 500-ns gate had negligible effects on the computer-generated data with a fast decay time of 40 μs. This indicates that the 500-ns sampling gate cannot contribute any observable artifacts to our experimental data. Furthermore, the transient difference spectra presented in this paper were compared with the data taken previously with a 100-ns gate (not presented here). The transient spectra taken with the shorter gate exhibited fast absorbance decay at 690 nm (in ~5 μs after photolysis) very similar to the data shown in Figure 3A. These results indicate that two fast dark reactions, attributed to the decays of two lumi-R intermediates, are present at the early stage of the phototransformation. We also performed a global analysis on the computer-generated data simulating the kinetic reactions involving five intermediates with the fast decay processes of 8 and 80 μs. The effects of the 500-ns gate on the rate constants of the early intermediates were found to be less than 5%, suggesting that the time resolution of our experiments was sufficient to measure the fast kinetic processes of the phytochrome phototransformation.

For the dark reactions in the late stage of the phototransformation, the apparent rate constants found in the present study correlate well with those observed in earlier studies.[19,26,34] In an approach similar to that described in the global data analysis section, Eilfeld and co-workers found that the phototransformation of native oat phytochrome in 20% glycerol was described by three kinetic processes with the time constants of 35.7 μs, 2.7 ms, and 50 ms at 298 K.[26] However, in their more recent study on the late steps of the phytochrome phototransformation, they observed an extra intermediate (designated as meta-Rac) between meta-Ra and meta-Rc in 66% (v/v) glycerol solvent.[34] They also reported that the time constant of the last reaction (meta-Rc to Pfr) was approximately 91 ms at 297 K in low glycerol content samples. More recently, Inoue and co-workers found that the phototransformation of native oat phytochrome consisted of four intermediates (not including the fast decay of lumi-R1 observed in this study) and that the time constant for the last dark reaction was approximately 167 ms at 297 K.[19] These authors found a "node" near 1.5 ms in their kinetic absorption data at 690 nm and attributed that to the formation of an additional intermediate (designated as meta-Rb′) between meta-Ra and meta-Rc. These results agree qualitatively with the conclusions of the current study which indicate that the later intermediates of the phototransformation decay with the apparent time constants of 7.6, 42, and at least 266 ms at 283 K. As we pointed out earlier (see Results), however, the time constant of the slowest dark reaction could be underestimated due to the lack of measurements at sufficiently long delay times.

It is not clear whether the additional intermediate in the late stage of the phototransformation found in this study and in ref 19 was observed by Eilfeld and co-workers[34] since they did not show the transient data at 690 nm from which Inoue et al. deduced the presence of meta-Rb′. As pointed out by Inoue et al.,[19] the discrepancy might be due to the fact that the spectral changes caused by the presence of the additional intermediate were rather

(49) Sarkar, H. K.; Moon, D.-K.; Song, P.-S. *Biochemistry* **1984**, *23*, 1882–1888.

small and could be easily obscured by the noise in the kinetic data. The difficulty in resolving this intermediate was also evident in our study, which found that, largely due to the similar spectra of meta-Rc and Pfr, the two slowest decay processes tended to appear as a single process which decayed with the average rate constant of the two processes. Note that the intermediate meta-Rac was only clearly resolved in a solvent of high microviscosity (66% glycerol by volume) rather than macroviscosity (33% Ficoll solution, weight to volume).[34] It is not clear whether this meta-Rac intermediate is correlated with meta-Rb′ found in the low-viscosity solvent (5% glycerol)[19] since the presence of meta-Rac could also be attributed to the interaction between the tetrapyrrole chromophore and solvent observed previously.[23] Both the transient spectra taken at 1.2 ms (Figure 6 in ref 19) and at 100 ms (in high glycerol concentration solution; see Figure 2 in ref 34) after photolysis show some resemblance to the absorption spectrum of meta-Ra2 in a simple sequential model (see Figure 6B). But as we pointed out earlier, these transient spectra could be mixed with the contribution of absorption of the intermediates other than meta-Rb′ or meta-Rac and could be interpreted by several kinetic models.

As shown in Figure 7, the first two intermediates, lumi-R1 and lumi-R2, appear to have very similar absorption spectra in the models with parallel pathways (Figure 5B,C). This is consistent with the common assumption made in the literature that the lumi-R intermediates that decay in parallel pathways should be equivalent in nature.[30,33,50] Because the model shown in Figure 5B b exhibits a considerably larger absorption spectrum of lumi-R2 compared to lumi-R1 (Figure 7B b), we consider this model less plausible than its counterpart shown in Figure 5B a (see Figure 7B a). The low-temperature absorption spectra could also be explained by the models with parallel pathways. In this case, both lumi-R1 and lumi-R1 could be trapped simultaneously at low temperatures. This is possible because lumi-R1 and lumi-R2 could have rather similar transition temperatures and therefore appear as a single intermediate in the low-temperature steady-state studies. In the sequential model (Figure 5A), the spectrum of lumi-R2 has a similar absorption maximum with reduced absorption intensity compared to that of lumi-R1 (Figure 7A). The absorption spectrum of lumi-R2 intersects the isosbestic point between the spectra of lumi-R1 and meta-Ra1 near 670 nm, and the shape of the spectrum of this intermediate seems normal. It is possible that an equilibrium could exist between the lumi-R1 and lumi-R2 intermediates at physiological temperature. Although we could not find additional experimental evidence to support this speculation, this would be consistent with the fact that the lumi-R2 intermediate is not observed in the low-temperature study.[18] As discussed in the global data analysis section, the low-temperature studies might not be able to trap all of the intermediates observed in time-resolved studies at physiological temperatures. If lumi-R1 and lumi-R2 form an equilibrium at physiological temperature (10 °C), then the lumi-R2 intermediate will not be observed at the very low temperatures (i.e., between −65 and −85 °C) at which the lumi-R1 to meta-Ra1 reaction takes place due to the fact that the free energy of lumi-R2 would be higher than that of lumi-R1 at the lower temperatures. Of course, it is also possible that the reaction from lumi-R1 to lumi-R2 is a simple sequential process without a back reaction. It could be difficult to resolve this reaction by low-temperature steady-state studies because the two lumi-R intermediates have similar absorption spectra.

Since the formation of Pfr must be a unbranched process, all of the models shown in Figure 5 exhibit almost identical absorption spectra of meta-Rc (see Figures 6B and 7), as explained previously. The absorption spectrum of meta-Rc is similar to that observed in low-temperature steady-state studies.[18] The spectra of the meta-Ra1 and meta-Ra2 intermediates appear to be very similar in parallel models (Figures 7B a and 7B b), and both spectra agree with that of the meta-Ra intermediate observed in low-temperature studies.[18] Therefore, the observation of the lumi-R, meta-Ra, and meta-Rc intermediates in the low-temperature steady-state studies can be easily explained by the assumption that lumi-R1 and lumi-R2, meta-Ra1 and meta-Ra2, and meta-Rc are each trapped at different low temperatures. If the dark reactions in the late stage of the phototransformation (meta-Ra → meta-Rc) proceed in a sequential pathway, then the shape of the meta-Ra2 spectrum derived from the unidirectional sequential model (Figure 6B) implies that meta-Ra2 is in equilibrium with meta-Ra1. The absorption spectrum of meta-Ra2 appears to be similar to that of meta-Rc when the equilibrium constant is 1.5. As explained in the global data analysis section, the meta-Ra2 intermediate (in Figure 5A) would not be trapped as a stable intermediate at any temperature. Therefore, the model shown in Figure 5A implies that the meta-Ra1 to meta-Rc transition observed at low temperatures would proceed through a slightly different pathway compared to that at physiological temperatures.

The alternative model shown in Figure 5C was first proposed by Eilfeld and co-workers to explain the presence of the meta-Rac intermediate observed in a high glycerol environment.[34] As shown in Figure 7C, the absorption spectrum of meta-Ra2 appears to be very similar to that of meta-Ra1 when the equilibrium constant between the two intermediates is 0.85. Despite the similarity of their absorption spectra, meta-Ra2 should be kinetically resolvable since the presence of this intermediate contributes an additional process to the kinetic decays to meta-Rc. At physiological temperatures meta-Ra1 is more favorable than meta-Ra2 in free energy, as illustrated by the fact that $k_{43} > k_{34}$ at 10 °C. This is necessary for the phototransformation to proceed to the later intermediates at higher temperatures. The opposite is true at low temperatures at which the meta-Ra2 intermediate is observed as a stable intermediate, i.e., meta-Ra2 should be lower in free energy relative to meta-Ra1. Therefore, according to the model shown in Figure 5C, it is the meta-Ra2 intermediate, rather than meta-Ra1, that is trapped at low temperatures. The stable equilibrium between meta-Ra1 and meta-Ra2 cannot be observed because, as the temperature is raised above the transition temperature between meta-Ra1 and meta-Rc (which is below the equilibrium temperature of the meta-Ra intermediates), meta-Rc would become energetically more favorable than meta-Ra2 and would be formed as a stable intermediate. It is not clear whether the meta-Ra2 intermediate in this model correlates with the meta-Rac or meta-Rb′ intermediate observed previously since the pure absorption spectra of these intermediates are not available.[19,34]

Implications about the Phototransformation Mechanism. We conclude from the global analysis of the laser photolysis data of native oat phytochrome at 10 °C that the phototransformation from Pr to Pfr involves five kinetic intermediates. It is possible to fit the transient absorption data with kinetic models having two parallel pathways or an unbranched sequential pathway. The formation of Pfr must be an unbranched reaction (meta-Rc → Pfr). If the dark transformation prior to meta-Rc is also a sequential process, our analysis indicates that the meta-Ra intermediates are in equilibrium. At present we consider the kinetic models illustrated in Figure 5A,B(a),C to be the likely candidates for the phototransformation of native oat phytochrome. Time-resolved absorption experiments at different temperatures should be useful for further examination of the equilibrium processes proposed by the sequential models shown in Figure 5A,C. The sequential models will be brought into question if the absorption spectra of the meta-Ra intermediates calculated from these models vary with temperature over a narrow range or if the true rate constants at different temperatures do not lead to linear Arrhenius behavior. If this were the case, the parallel models might be more favored compared to the sequential models. It is not clear whether the partition constants of the two parallel pathways should depend on temperature. The fraction of the reaction proceeding through each pathway should be temperature independent if the parallel reactions are due to the heterogeneity of the phytochrome sample, as proposed in previous studies.[33,50] However, it is also possible that the decay of the primary intermediate (i.e., prelumi-R; see ref 20) is split into two branches in which the partition constants could be strongly temperature dependent. Time-resolved ab-

(50) Pratt, L. H.; Shimazaki, Y.; Inoue, Y.; Furuya, M. *Photochem. Photobiol.* **1982**, *36*, 471–477.

sorption studies at different temperatures should further resolve the kinetic mechanism of the phytochrome phototransformation.

The transient spectra shown in Figure 8 indicate that the changes in the near-UV and blue spectral regions of the pigment are consistent with those of the visible band at different stages of the phototransformation from Pr to Pfr. The absorption band of the chromophore in this spectral region undergoes a red shift in the early stage of the phototransformation due to the formation of the lumi-R intermediates. The fact that the transient spectrum taken at 1 ms is almost identical to that at 100 μs is consistent with the apparent rate constants obtained from the kinetic measurements in the visible band, which indicate that the phytochrome phototransformation can be divided into the early and late stages. As shown in Figure 8, the absorption spectrum of the chromophore undergoes an additional red shift during the late stage of the phototransformation, resembling the spectral changes in the visible band at these times. These dramatic spectral changes can be induced by the movement of charged residue(s) in the vicinity of the tetrapyrrole chromophore, as demonstrated by the results of molecular orbital calculations.[51-53] The conformational changes of native oat phytochrome at the different stages of the phototransformation have also been studied by time-resolved circular dichroism measurements in the red spectral region.[45]

A particularly interesting feature of the transient difference spectra shown in Figure 8A is the appearance of a difference absorption band near 315 nm in the late stage of the phototransformation (after 1 ms). The nature of this absorption band is not clear. It could be due to the absorption of the aromatic amino acid residue(s) or a "forbidden" band of the chromophore. More specifically, this band could be due to the absorption of a tyrosinate residue(s). Although tyrosinate is believed to absorb near 295 nm, it seems possible that this absorption band could undergo a red shift (by 20 nm) in ionic or charged environments. Photolysis studies of CO-bound hemoglobin also found a small increase in the transient absorption near 320 nm accompanied by a bleaching around 270 nm.[54] If this assignment is appropriate, our results indicate that deprotonation of a tyrosine residue(s) occurs during the late stage of the phototransformation. This would corroborate the earlier observation of the proton release in the phototransformation of pea phytochrome from Pr to Pfr at basic pH.[16,55] On the other hand, the open tetrapyrrole chromophore in phytochrome has a complicated structure and can contribute to the absorption near 315 nm. It was found in light-adapted bacteriorhodopsin that the pigment exhibited rather intense CD but insignificant absorption bands in this region.[56] This suggests that the chromophore in phytochrome could also have a "forbidden" absorption band in this region which could be partially allowed in the late stage of the phototransformation due to the changes of the chromophore conformation as well as the electrostatic environment. This assignment would be supported by the previous kinetic measurements which indicated that the late stage of the phototransformation was significantly retarded in viscous solvents[34] and by the linear dichroism measurements which showed large changes in the chromophore orientation during the phototransformation.[57] In any event, the appearance of the distinct absorption band near 315 nm after 1 ms is an additional indication of large chromophore or protein conformational changes in the late stage of the phototransformation.

It seems from the above discussion that the various phenomena of potential physiological importance, such as the deprotonation of the chromophore and possibly of the tyrosine residue(s), the large change of the chromophore orientation, and dramatic changes of chromophore and protein conformations, are all correlated with the late stage of the phototransformation. These phenomena should be better resolved by photolysis measurements of the absorption and the circular dichroism in the UV spectral region and the linear dichroism of the chromophore absorption band. Work is currently in progress to perform these time-resolved experiments for more definitive assignment of the spectral changes in the phytochrome phototransformation.

Acknowledgment. We thank Dr. J. W. Lewis and T. E. Thorgeirsson for helpful discussions and the National Institutes of Health for support of this work through Grants GM-35158 (to D.S.K.) and GM-36956 (to P.S.S.). This work was also supported by a Maude-Hammond-Fling Travel Award (to D.L.F.).

(51) Suzuki, H.; Sugimoto, T.; Ishikawa, K. *J. Phys. Soc. Jpn.* **1975**, *38*, 1110–1118.
(52) Sugimoto, T.; Ishikawa, K.; Suzuki, H. *J. Phys. Soc. Jpn.* **1976**, *40*, 258–266.
(53) Sugimoto, T.; Inoue, Y.; Suzuki, H.; Furuya, M. *Photochem. Photobiol.* **1984**, *39*, 697–702.
(54) Björling, S. C. Ph.D. Dissertation, University of California, Santa Cruz, CA, 1991.
(55) Tokutomi, S.; Yamamoto, K. T.; Furuya, M. *Photochem. Photobiol.* **1988**, *47*, 439–455.
(56) Muccio, D. D.; Cassim, J. Y. *J. Mol. Biol.* **1979**, *135*, 595–609.
(57) Ekelund, N. G. A.; Sundqvist, C.; Quail, P. H.; Vierstra, R. D. *Photochem. Photobiol.* **1985**, *41*, 221–223.